

# Rapid Bonding of $\text{Ti}_3\text{SiC}_2$ and $\text{Ti}_3\text{AlC}_2$ by Pulsed Electrical Current Heating

Lu Shen,<sup>‡</sup> Jianming Xue,<sup>§</sup> Michel W. Barsoum,<sup>¶</sup> and Qing Huang<sup>‡,†</sup>

<sup>‡</sup>Division of Functional Materials and Nanodevices, Ningbo Institute of Materials Technology and Engineering, Chinese Academy of Sciences, Ningbo, Zhejiang 315201, China

<sup>§</sup>State Key Laboratory of Nuclear Physics and Technology, Peking University, Beijing 100871, China

<sup>¶</sup>Department of Materials Science and Engineering, Drexel University, Philadelphia, Pennsylvania 19104

Inspired by pressure resistance welding of metallic materials, herein we describe how two MAX phases— $\text{Ti}_3\text{SiC}_2$  and  $\text{Ti}_3\text{AlC}_2$ —were successfully joined by a rapid electric current heating method in a pulsed electric current sintering furnace. No welding agent was employed and the total processing time was less than 6 min. When the bulk temperature of the joint couple exceeded  $1070^\circ\text{C}$ , good joints, with shear strength above 50 MPa, were achieved in both homo- and heterojunction joints.

## I. Introduction

SOME MAX phases materials, mainly  $\text{Ti}_3\text{SiC}_2$ ,  $\text{Ti}_3\text{AlC}_2$ , and  $\text{Ti}_2\text{AlC}$ , are promising structural materials in nuclear and other high-temperature applications due to their excellent mechanical properties,<sup>1,2</sup> corrosion resistance,<sup>3,4</sup> moderate irradiation tolerance,<sup>5,6</sup> and good oxidation resistance properties.<sup>7,8</sup> To realize their potential, large and/or complex-shaped components fabrication techniques, such as gel-casting, slip-casting as well as joining need to be developed. In general less attention has been paid to joining of MAX phases than has been devoted to understanding their properties. The former is crucial in the nuclear materials area as the joint interface is almost always the source of failures (fatigue crack growth, stress-induced damage, low oxidation resistance, gas or toxic nuclide leakage, etc.).<sup>9</sup>

In general, joining of structural ceramics can be achieved using an inert or reactive filler material. The former includes eutectic alloys<sup>10</sup> or glasses<sup>11</sup> that join through surface wetting and capillarity force; the latter reacts with the matrix to form transition layers.<sup>12</sup> However, the presence of an interlayer phase or residual metals and alloys at the interface could create problems if they were less resistant to corrosion or oxidation, or more susceptible to neutron irradiation.

In the case of the MAX phases, Yin *et al.* have shown the effectiveness of joining of  $\text{Ti}_3\text{SiC}_2$  and  $\text{Ti}_3\text{AlC}_2$  polycrystalline samples by introducing reactive interlayers of Al or Si, respectively.<sup>13,14</sup> The same group reported on direct diffusion bonding between  $\text{Ti}_3\text{SiC}_2$  and  $\text{Ti}_3\text{AlC}_2$ .<sup>15</sup> However, these methods require relatively long annealing times (30–120 min) because the entire assembly needs to be heated to the joining temperatures ( $1200^\circ\text{C}$ – $1300^\circ\text{C}$ ).

Recently, a pressure resistance welding (PRW) technique was developed to seal Zr-alloy cladding tubes in the nuclear

fuel field.<sup>16</sup> During PRW, Joule heat builds up at the higher electrical resistance contact surfaces in tens of milliseconds when an electrical current passes through, which locally accelerates self-diffusion and promotes bonding. The application of some pressure during the process promotes plastic deformation and ensures good contact between the surfaces that are being joined.

Pulsed electric current sintering (PECS; sometimes referred to the spark plasma sintering) has been widely employed to fabricate ceramics with fine-grained microstructures which are difficult to densify by conventional methods. This method takes advantage of the fast, current-induced Joule heating of the graphite dies and the unidirectional load applied. Therefore, a PECS facility may be a suitable platform to test the feasibility of joining of conductive ceramics such as the MAX phase. In fact,  $\text{ZrB}_2$ -SiC composites have been successfully joined at  $1800^\circ\text{C}$  in 300 s in a PECS furnace, using a Zr-B filler. Room and high-temperature ( $1350^\circ\text{C}$ ) shear strengths, as well as, the oxidation behavior of the joined substrates were found to be equal to the base-line substrates.<sup>17</sup>

The aim of this work was to apply the PRW concept to the joining of  $\text{Ti}_3\text{SiC}_2$  and  $\text{Ti}_3\text{AlC}_2$ , henceforth referred to as TSC and TAC, respectively, to themselves and to each other in a PECS furnace. The resulting microstructures and the shear strengths of the joints were evaluated.

## II. Experimental Details

Commercial TSC and TAC 300 mesh powders, with a purity of 98 wt % according to the provider (Beijing Jinhezhi Materials Co., Ltd., Beijing, China) were used as starting materials. The main impurity phases in the TSC powders were TiC and  $\text{TiSi}_2$ ; in TAC, it was  $\text{Al}_2\text{O}_3$ . The prereacted  $\text{Ti}_3\text{SiC}_2$  powders were sintered at  $1330^\circ\text{C}$  for 600 s using a load corresponding to a uniaxial pressure of 35 MPa. The prereacted  $\text{Ti}_3\text{AlC}_2$  powders were also PECS sintered at  $1260^\circ\text{C}$  for 600 s using a load corresponding to a uniaxial pressure of 28 MPa. The relative bulk densities of the as-sintered TSC and TAC samples measured by Archimedes principle were 98.5% and 98.9%, respectively. The sintered samples were electrodischarged, machined, EDMed, into  $17\text{ mm} \times 17\text{ mm} \times 5\text{ mm}$  parallelepipeds. The surfaces to be joined were sanded and polished with sandpaper from 400# to a final one of 2000#. Before joining, the surfaces were cleaned with ethanol.

The following couples—TSC–TSC, TAC–TAC, and TSC–TAC, were placed between two graphite punches in the center of a PECS furnace (FCT, HP 25, Germany) cavity as shown in Fig. 1(a). The joining temperature ( $T_j$ ) was monitored and controlled by a pyrometer placed on the top, which measured the inner bottom surface of the top graphite

D. Marshall—contributing editor

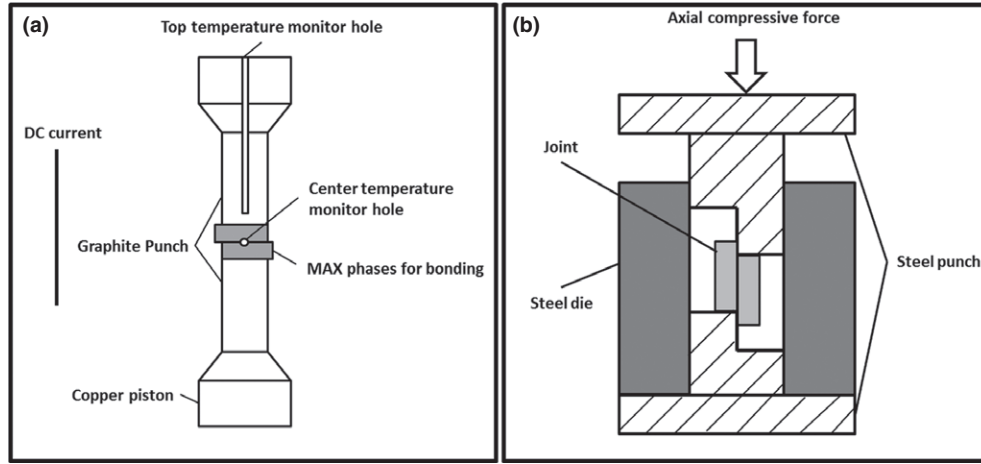


Fig. 1. Scheme of the, (a) bonding setup, and (b) shear strength test assembly.

punch (the graphite punch designed by FCT was a tubular one). The actual bulk temperature ( $T_B$ ) at, or near, the interface of the joint was recorded by a second pyrometer (not shown in Fig. 1). Three temperatures ( $T_J$ ), 1150°C, 1200°C, and 1300°C, were used for joining. A load corresponding to a contact pressure of 15 MPa was applied. At temperatures  $>450^\circ\text{C}$ , the heating rate used was about 2.5 K/s. Once  $T_J$  was reached, the current was turned off immediately and the assembly was allowed to cool in the PECs furnace. The entire joining process, from start to finish, lasted  $<6$  mins.

The joint quality was determined by measuring its interfacial shear strengths using a laboratory made assembly shown in Fig. 1(b). The details can be found in Ref. [18] The shear strength was calculated by the equation assuming,  $\tau = P/S$ , where  $\tau$  is the shear strength (MPa),  $P$  is the maximum load (N), and  $S$  the bonding area ( $\text{mm}^2$ ). Three joints at each temperature were tested and their average and maximum deviations were calculated.

### III. Results and Discussion

The maximum  $T_B$  recorded by the pyrometer focused on the interfacial area, as well as, the maximum currents applied during the bonding process as listed in Table I. From these results, it is clear that  $T_B$  was about  $100^\circ\text{C}$ – $200^\circ\text{C}$  lower than  $T_J$ . All else being equal,  $T_J$  and  $T_B$  of the TAC–TAC couple were the highest, those for the TSC–TSC joint the lowest, with those for the TSC–TAC couple in between. This difference most probably reflects the fact that the interfacial resistances of the TAC samples were higher than their TSC counterparts. In the remainder of this letter, the discussion will refer to  $T_B$  because that value is closer to the true interfacial temperature. Note that actual interfacial temperature is probably higher. A current of  $\approx 1.2$  KA, equivalent to a current density of about  $470 \text{ A/cm}^2$  on the joint face, was enough to provide the temperature rise for all the joints.

When the average joints' shear strengths are plotted versus  $T_B$  (Fig. 2), two regimes can be discerned. At  $T_B$ 's

below  $\sim 1075^\circ\text{C}$ , the average shear strengths of the joints were at or  $<40$  MPa. The TSC–TSC joint, bonded at  $\sim 1023^\circ\text{C}$ , exhibited the lowest average shear strength ( $< 20$  MPa). The failure was typically located at the interface, indicating poor bonding. At around 40 MPa, the average shear strengths of the TSC–TAC joint bonded at  $\sim 1035^\circ\text{C}$  was comparable to that of the TSC–TSC joint bonded at  $1050^\circ\text{C}$ . Note that the shear strengths of the TSC–TAC joints were quite scattered, which most probably reflected partial bonding in some areas. Both joints had a complex failure pattern, where the cracks meandered from the interface into the bulk.

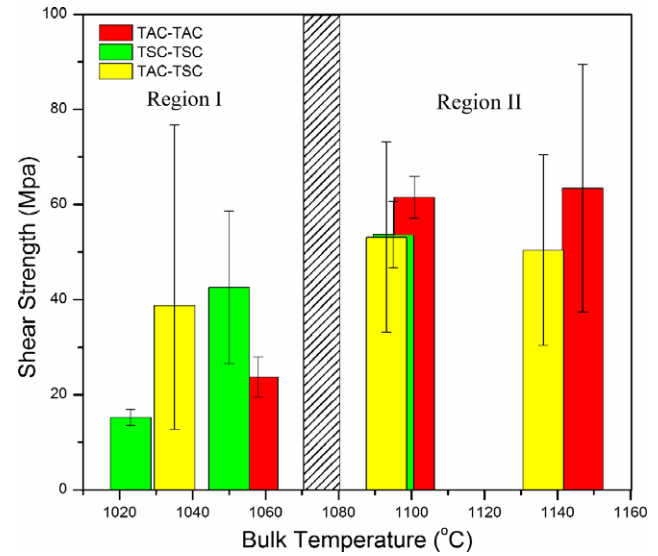
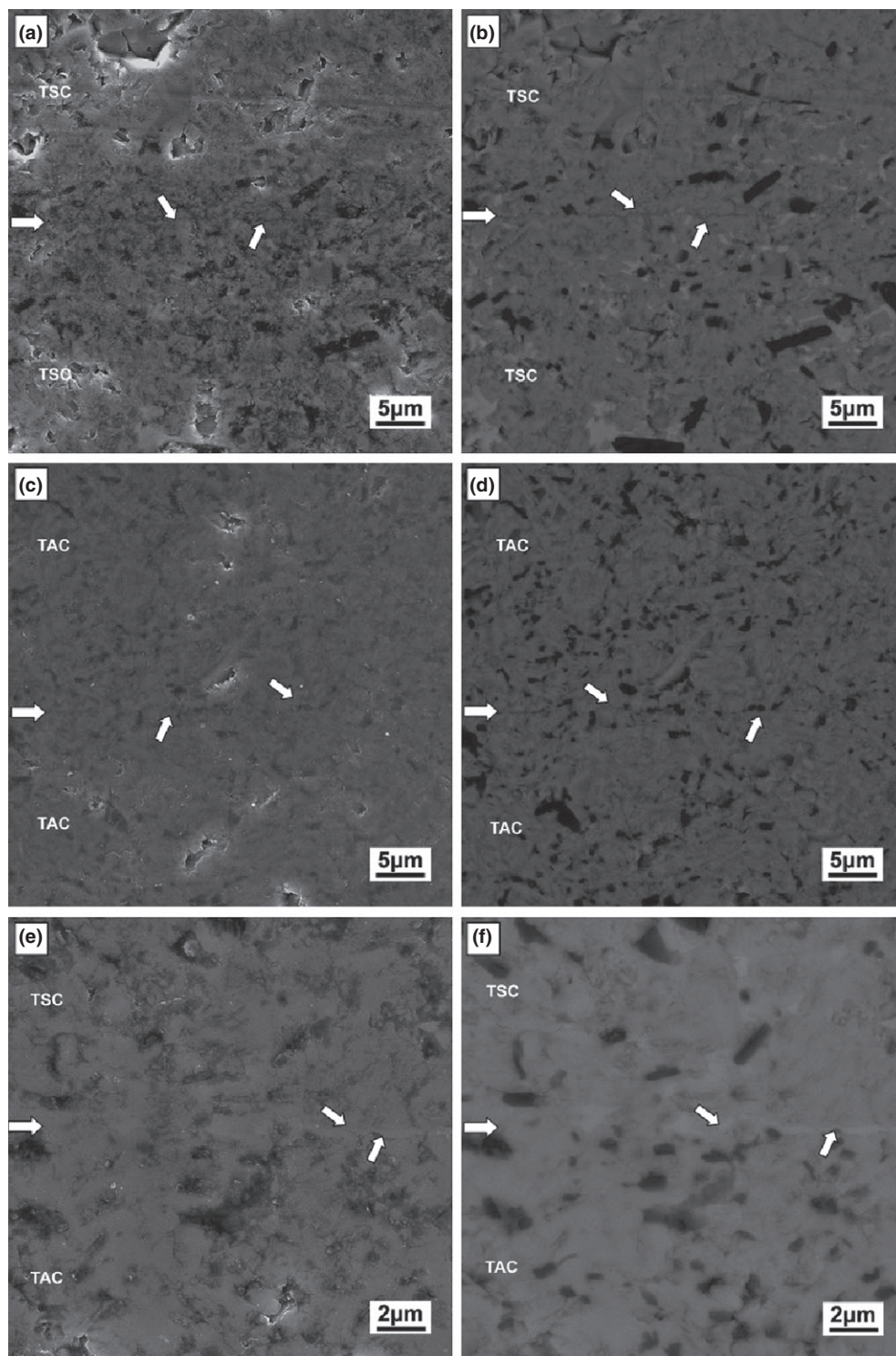


Fig. 2. Shear strengths of the bonded joints. The error bars indicate the maximum deviation from average.

Table I. Joining Parameters ( $T_B$  and max current  $I_M$ ) and Shear Failure Location of TSC–TSC, TAC–TAC, and TSC–TAC Joining Couples

$T_J$ (°C)	TSC–TSC			TAC–TAC			TSC–TAC		
	$T_B$ (°C)	$I_M$ (KA)	Location	$T_B$ (°C)	$I_M$ (KA)	Location	$T_B$ (°C)	$I_M$ (KA)	Location
1150°C	~1023	~1.21	I	~1059	~1.16	I	~1035	~1.14	B + I
1200°C	~1050	~1.17	B + I	~1110	~1.18	B <sub>(mainly)</sub> + I	~1092	~1.18	B <sub>(mainly)</sub> + I
1300°C	~1095	~1.30	B	~1148	~1.32	B	~1135	~1.24	B

I, Shear fracture at joint interface; B, Shear fracture in bulk.



**Fig. 3.** Typical SEM images of polished cross-sections of joints: (a) TSC–TSC in secondary electron (SE) mode, (b) TSC–TSC in BSE mode, (c) TAC–TAC in SE mode, (d) TAC–TAC in backscatter electron (BSE) mode, (e) TSC–TAC in SE mode, (f) TSC–TAC in BSE mode. In all figures the broad white arrows indicate the location of the original interfaces.

When the average interfacial strengths of the various couples in region I are compared (Fig. 2) it is clear that in general the TAC–TAC joints needed higher temperatures to achieve the same interface strengths as those that contained TSC.

In region II, where the  $T_B$ 's were  $>1080^\circ\text{C}$ , the shear strengths of all the joints were quite respectable and were independent of the bonding temperatures. The average shear strengths of the TAC–TAC joints was centered at about 63 MPa, whereas for the TSC–TSC joint and TSC–TAC joints, the shear strength averaged about 52 MPa. The lower

strengths for the latter, probably reflect the fact that the shear strengths of the bulk TAC samples used herein was about 60 MPa, whereas those of TSC bulk were 50 MPa. In other words, the joint shear strengths were at least as strong as, if not stronger than, the bulk material, which in turn explains why most failures occurred in the bulk and away from the interface. In other words, the shear strengths of the bulk materials determined the strengths.

To gain further insight in the bonding mechanism, the joints were cross-sectioned, mounted and polished, and observed in a SEM. Remarkably, and for the most part, it



was difficult to locate the original interfaces in secondary electron (SE) SEM images [Figs. 3(a), (c) and (e)]. Careful examination in backscatter electron (BSE) mode in the SEM, however, revealed the existence of a faint bonding line [wide white arrows in Figs. 3(b), (d) and (f)].

When the TSC–TAC joint was imaged in BSE [Fig. 3(f)] mode in the SEM, a thin, slightly brighter, layer was observed at the bonding interface. The exact nature of this layer remains unclear at this time. Yin *et al.* reported the formation of  $\text{Ti}_5\text{Si}_3$  at the interface of TSC–TAC joint from XRD and TEM observations.<sup>15</sup> However, in their work, the joining was conducted by longtime diffusion method, which provided enough time for equilibrium phase formation. Considering the rapid processing of this study, whether this layer is  $\text{Ti}_5\text{Si}_3$  needs further work.

#### IV. Conclusion

In this study, we successfully bonded  $\text{Ti}_3\text{SiC}_2$  and  $\text{Ti}_3\text{AlC}_2$  to themselves and to each other by passing an electric current through the joint interfaces. This process has several advantages: it is rapid and energy efficient. It opens the door for using the PRW technique adopted in sealing nuclear fuel cladding tubes to the MAX phases.

In summary, TSC–TSC, TAC–TAC, and TSC–TAC couples were successfully joined by a pressure resistance joining process in a pulse electric current sintering furnace. The electric current density used was about  $470 \text{ A/cm}^2$ , which resulted in a bulk temperature of about  $1100^\circ\text{C}$ . Good joints, with average shear stresses of between 50 and 60 MPa were produced within a total bonding time of less than 6 min.

#### References

- <sup>1</sup>M. W. Barsoum, *MAX Phases: Properties of Machinable Carbides and Nitrides*. Wiley VCH GmbH & Co., Weinheim (2013).
- <sup>2</sup>M. W. Barsoum and M. Radovic, “Elastic and Mechanical Properties of the MAX Phases,” *Annu. Rev. Mater. Res.*, **41**, 195–227 (2011).

- <sup>3</sup>J. Xie, X. Wang, A. Li, F. Li, and Y. Zhou, “Corrosion Behavior of Selected  $\text{M}_{n+1}\text{AX}_n$  Phases in Hot Concentrated HCl Solution: Effect of a Element and MX Layer,” *Corros. Sci.*, **60**, 129–35 (2012).
- <sup>4</sup>L. Li, G. Yu, and X. Zhou, “Corrosion Behaviour of  $\text{Ti}_3\text{SiC}_2$  and  $\text{Ti}_3\text{AlC}_2$  with LiF–NaF–KF Molten Salt,” *Nucl. Tech.*, **37** [6] 060602, 6pp (2014).
- <sup>5</sup>E. N. Hoffman, D. W. Vinson, R. L. Sindelar, D. J. Tallman, G. Kohse, and M. W. Barsoum, “MAX Phase Carbides and Nitrides: Properties for Future Nuclear Power Plant in-Core Applications and Neutron Transmutation Analysis,” *Nucl. Eng. Des.*, **244**, 17–24 (2012).
- <sup>6</sup>S. Zhao, J. Xue, Y. Wang, and Q. Huang, “*Ab Initio* Study of Irradiation Tolerance for Different  $\text{M}_{n+1}\text{AX}_n$  Phases:  $\text{Ti}_3\text{SiC}_2$  and  $\text{Ti}_3\text{AlC}_2$ ,” *J. Appl. Phys.*, **115** [2] 023503, 9pp (2014).
- <sup>7</sup>H. B. Zhang, Y. C. Zhou, Y. W. Bao, and M. S. Li, “Improving the Oxidation Resistance of  $\text{Ti}_3\text{SiC}_2$  by Forming a  $\text{Ti}_3\text{Si}_{0.9}\text{Al}_{0.1}\text{C}_2$  Solid Solution,” *Acta Mater.*, **52** [12] 3631–7 (2004).
- <sup>8</sup>X. H. Wang and Y. C. Zhou, “Oxidation Behavior of  $\text{Ti}_3\text{AlC}_2$  at 1000–1400°C in Air,” *Corros. Sci.*, **45** [5] 891–907 (2003).
- <sup>9</sup>Y. Katoh, L. L. Snead, T. Cheng, C. Shih, W. D. Lewis, T. Koyanagi, T. Hinoki, C. H. Henager Jr., and M. Ferraris, “Radiation-Tolerant Joining Technologies for Silicon Carbide Ceramics and Composites,” *J. Nucl. Mater.*, **448** [1–3] 497–511 (2014).
- <sup>10</sup>Y. Liu, Z. Huang, and X. Liu, “Joining of Sintered Silicon Carbide Using Ternary Ag–Cu–Ti Active Brazing Alloy,” *Ceram. Int.*, **35** [8] 3479–84 (2009).
- <sup>11</sup>M. Ferraris, M. Salvo, V. Casalegno, A. Ciampichetti, F. Smeacetto, and M. Zucchetti, “Joining of Machined SiC/SiC Composites for Thermonuclear Fusion Reactors,” *J. Nucl. Mater.*, **375** [3] 410–5 (2008).
- <sup>12</sup>Y.-I. Jung, S.-H. Kim, H.-G. Kim, J.-Y. Park, and W.-J. Kim, “Microstructures of Diffusion Bonded SiC Ceramics Using Ti and Mo Interlayers,” *J. Nucl. Mater.*, **441** [1–3] 510–3 (2013).
- <sup>13</sup>N. Jerred, L. Zirker, B. Jacques, T. Bradshaw, J. Carrillo, E. Young, I. Charit, J. Cole, M. Frary, D. Butt, M. Meyer, and K. L. Murty, Pressure Resistance Welding of High Temperature Metallic Materials, INL/CON-10-17975, 2010.
- <sup>14</sup>X. Yin, M. Li, and Y. Zhou, “Microstructure and Mechanical Strength of Transient Liquid Phase Bonded  $\text{Ti}_3\text{SiC}_2$  Joints Using Al Interlayer,” *J. Eur. Ceram. Soc.*, **27** [12] 3539–44 (2007).
- <sup>15</sup>X. Yin, M. Li, T. Li, and Y. Zhou, “Diffusion Bonding of  $\text{Ti}_3\text{AlC}_2$  Ceramic via a Si Interlayer,” *J. Mater. Sci.*, **42** [17] 7081–5 (2007).
- <sup>16</sup>X. Yin, M. Li, J. Xu, J. Zhang, and Y. Zhou, “Direct Diffusion Bonding of  $\text{Ti}_3\text{SiC}_2$  and  $\text{Ti}_3\text{AlC}_2$ ,” *Mater. Res. Bull.*, **44** [6] 1379–84 (2009).
- <sup>17</sup>W. R. Pinc, M. Di Prima, L. S. Walker, Z. N. Wing, and E. L. Corral, “Spark Plasma Joining of  $\text{ZrB}_2$ –SiC Composites Using Zirconium–Boron Reactive Filler Layers,” *J. Am. Ceram. Soc.*, **94** [11] 3825–32 (2011).
- <sup>18</sup>J. Wang, K. Li, W. Li, H. Li, Z. Li, and L. Guo, “The Preparation and Mechanical Properties of Carbon/Carbon Composite Joints Using Ti–Si–C Filler as Interlayer,” *J. Mater. Sci. Eng., A*, **574**, 37–45 (2013). □